An Islanding Detection Algorithm for Inverter-based Distributed Generation Based on Reactive Power Control

Xiaolong Chen, Yongli Li

***Abstract*—For the inverter-based distributed generation (DG) under constant power control, this paper analyzes the relationship between the active/reactive power mismatch and frequency deviation respectively during islanding and finds that the frequency variation trends caused by active and reactive power mismatches may be opposite. In order to eliminate the nondetection zone (NDZ) and detect islanding rapidly, an innovative islanding detection algorithm is presented based on a reactive power control strategy. The strategy provides the reactive power reference for the DG to guarantee the consistency of the frequency variation trends caused by both active and reactive power mismatches, thus accelerating the islanding detection speed. In addition, the introduction of the voltage variation into the proposed reactive power control strategy can regulate voltage dynamically in grid-connected mode and further shorten the islanding detection time as well. According to the anti-islanding test system in the IEEE Std.929-2000 and IEEE Std.1547-2003, several case studies are carried out in the power systems computer-aided design (PSCAD) /EMTDC environment. The simulation results show that the proposed algorithm has the zero NDZ property and can detect islanding rapidly. Moreover, the algorithm also performs effectively for load imbalance conditions as well as for the system with multiple DGs.**

***Index Terms*—Inverter-based distributed generation, islanding detection, reactive power control strategy, power factor improvement, voltage regulation.**

I. INTRODUCTION

THE application of distributed generation (DG) in the distribution system to supply electric power for the network and local load is growing rapidly. Using renewable energy sources such as photovoltaic (PV) generation, wind power, fuel cell and microturbine to produce power, the DG brings technical, environmental and economic benefits for utilities and customers [1], [2]. However, there are also challenges associated with the DG [2], among which islanding detection is an important and difficult one.

Manuscript received March 07, 2013; revised April 29, 2013 and August 20, 2013; accepted September 18, 2013. This work was supported in part by the Project supported by the National Basic Research Program of China (973 Program) under Award Number 2009CB219704, and in part by the Program of National Natural Science Foundation of China under Award Number 51177108.

The authors are with the Department of Electrical Engineering and Automation, Tianjin University, Tianjin 300072, China (e-mail: promising1207@163.com; lyltju@163.com).

According to the IEEE Std.929-2000, islanding is a condition in which a portion of the utility system that contains both the DG and load continues operating while this portion is electrically separated from the main utility [3]. There are two types of islanding: intentional islanding and inadvertent islanding. According to the control strategy in advance, intentional islanding forms in a controlled manner to make good use of the DG and improve the power supply reliability [4], [5]. This operation mode is not studied in this paper. On the contrary, inadvertent islanding can lead to power quality problems, serious equipment damage, and even safety hazards to utility operation personnel [6]. Therefore, the DG has to detect islanding rapidly and effectively in this case and disconnect itself from the network as soon as possible to prevent the damages mentioned above. A generic system for islanding detection study is recommended in the IEEE Std. 929-2000 and IEEE Std. 1547-2003, where the distributed network, a RLC load and an inverter-based DG are connected at the point of common coupling (PCC).

Generally, there are mainly three types of islanding detection methods including communication-based, passive and active methods. Though communication-based methods do no harm to the power quality of the power system with the negligible nondetection zone (NDZ), the cost is much higher than the other two types of methods and the operations are more complex as well [7]. Therefore, passive and active methods have been well developed so far. Over/under frequency protection (OFP/UFP), over/under voltage protection (OVP/UVP) and phase jump detection (PJD) are the most widely used passive islanding detection methods, which determine the islanding condition by measuring the PCC voltage and the current from the DG [8]. These passive methods have cost and technology neutral merits, but they may fail to detect the islanding operation when the local load consumption closely matches the DG output [9]. On the other hand, active methods rely on injecting intentional disturbances or harmonics into some DG parameters to identify whether islanding has occurred [10]-[12]. The active frequency drift (AFD) [13], Slip-mode frequency shift (SMS) [14] and Sandia frequency shift (SFS) [15] methods are three classical active methods by creating a continuous trend to change the frequency during islanding. Though active methods suffer smaller NDZs, the presence of disturbances during normal operation will sacrifice

power quality and reliability of the power system. Moreover, when applied in multiple-DG operation, some active methods have difficulty in maintaining synchronization and may not work owing to the averaging effect [16]-[18].

It is common in conventional distribution systems that bus voltage drops below the limit especially at the remote end of the feeders or for heavy load, whereas the feeder node voltage may also suffer overvoltage due to the reverse power flow with the increasing DG penetration level. For the grid with high X_g/R_g lines (The grid is represented by an infinite voltage source with an equivalent line impedance $R_g + jX_g$), reactive power injection is most effective to improve voltage profile [19]. On the other hand, the reactive power mismatch can drive the frequency of the PCC voltage to change during islanding. Therefore, several studies have utilized the reactive power output capability of the DG to detect islanding as well as regulate the PCC voltage.

The DG operating at a unity power factor under constant power control means that it generates active power with all its capacity during the normal operation. The islanding detection methods proposed in [20]-[23] were designed for this kind of DG. Reference [20] presented an islanding detection method relying on equipping the DG interface with a *Q-f* characteristic. The DG *Q-f* characteristic was represented by a linear function where the slope was adjusted to be steeper than that of the load curve. Thus, the reactive power mismatch would force the frequency of the PCC voltage to deviate outside the thresholds during islanding. However, the slope of the load *Q-f* curve was dependent on the load active power consumption, the load's resonant frequency and quality factor. The load's resonant frequency and quality factor were unknown in advance and the load active power consumption might change during islanding because of the active power mismatch. Therefore, it was hard to guarantee that the slope of the DG *Q-f* curve, which was a preset and fixed value, would be steeper than that of the load curve. In addition, the meeting point of the two curves might exist within the frequency limits and the method would fail to detect islanding when the islanding occurred at the meeting point. An autonomous controller was proposed in [21] with integrated voltage regulation and islanding detection for high penetration PV applications. Though fast voltage regulation and coordination of multiple-PV systems to detect islanding could be realized, the islanding detection still suffered the NDZ with the complex controller. An islanding detection method based on intermittent bilateral reactive power variation was proposed in [22]. The frequency was forced to deviate outside the normal range during islanding through controlling the DG output reactive power to vary. The variation amplitude depended on the DG output active power and the load quality factor. Compared with the method in [22], the proposed method in [23] was improved by only outputting unilateral reactive power variation in each variation period and reducing the injected reactive power based on the load's resonance frequency detection. However, the load quality factor was unknown in advance. If the islanding occurred when the reactive power variation was equal to zero, it would not be detected rapidly with the detection time probably up to a whole variation period. Moreover, when the methods were applied to multiple DGs, the synchronization of the reactive power variation could not be guaranteed and the effectiveness of the methods might be reduced.

When the local load has high consumption of reactive power, additional conductor and transformer capacity is required to maintain the load power factor and the utility company suffers large energy lost. To solve these problems with its potential advantages, the DG integrated in the distribution feeder was also explored to compensate reactive power simultaneously for power factor improvement [24], [25], as well as the voltage regulation [19], [26]. Nevertheless, this could also enlarge the NDZ of the OFP/UFP method and make the islanding detection more difficult compared with the condition that the DG operated at a unity factor [27]. An islanding detection method was designed in [27] for this kind of DG by continuously and partly compensating the load reactive power consumption. Thus, the reactive power mismatch would force the frequency to rise for the inductive load and drop for the capacitive load until the frequency deviated outside the OFP/UFP limits. However, the reactive power mismatch was dependent on the load reactive power consumption. The detection speed varied and it was too slow for the load that consumed little reactive power. The impact of the active power mismatch on the frequency deviation was not considered as well, which also might make the islanding detection slow. In addition, according to the method, the grid always injected reactive power for the inductive load or absorbed reactive power for the capacitive load in grid-connected mode, which could not regulate the PCC voltage dynamically. Therefore, an innovative islanding detection algorithm is proposed in this paper for this kind of the DG.

The frequency of the PCC voltage eventually deviates to the resonant frequency during islanding when the DG operates at a unity power factor. Thus, the active power mismatch only forces the PCC voltage to change. However, the impact of the active power mismatch on frequency deviation has to be considered for the DG generating reactive power. This paper investigates the relationship between the active/reactive power mismatch and the frequency variation respectively during islanding and finds that the frequency variation trends caused by active and reactive power mismatches are opposite in some cases. Therefore, the frequency variation caused by the active power mismatch may be offset by that caused by the reactive power, which makes the islanding detection hard and slow. In order to eliminate the NDZ and detect islanding rapidly, this paper presents an innovative islanding detection algorithm based on a reactive power control strategy. According to the load reactive power consumption, the PCC voltage and its frequency, the corresponding reactive power reference is provided for the DG to make the frequency variation trend caused by the reactive power mismatch keep the same as that caused by the active power mismatch. The frequency continues to rise or drop and eventually deviates outside the limits of the OFP/UFP scheme in a very short time. In addition, the voltage variation is also introduced into the proposed strategy for two purposes: 1) Enlarging the reactive power mismatch and further

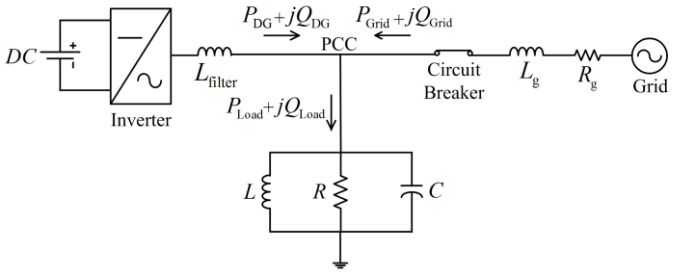

Fig. 1. System for islanding detection study.

shortening the detection time during islanding; 2) Regulating the PCC voltage dynamically in grid-connected mode through controlling the DG to generate different amounts of reactive power. Therefore, the proposed reactive power control strategy can take full advantage of the DG by integrating fast islanding detection, load power factor improvement and voltage regulation.

II. System Modeling and Basic Relationship Analysis

According to the IEEE Std.929 and IEEE Std.1547, the recommended generic system for islanding detection study is shown in Fig. 1. It consists of an inverter-based DG, a parallel three-phase RLC load and the distributed network represented by a three-phase source behind impedance. The DG is usually located near the local load and the length of the line connecting them is short. Therefore, the line loss is negligible and the RLC load and the DG are connected at the PCC in the generic system. Moreover, the DGs such as PV generation and wind power generation are usually configured with the maximum power point tracking controller. The output power can be considered to be constant during the detection because the detection time is very short. Therefore, using a constant dc source behind a three-phase inverter, the DG is designed as a constant power source to control the active and reactive power independently based on the dual close loop control structure in the d-q synchronous reference frame. According to the instantaneous power theory and the Park transformation, the instantaneous active and reactive power of the DG output can be written in terms of the d-q axis components as follows [28]:

$$P_{DG}=\frac{3}{2}u_d i_d \tag{1}$$

$$Q_{DG}=\frac{3}{2}u_d i_q \tag{2}$$

where u_d and u_q are the d-q components of the voltage at the PCC, and i_d and i_q represent the d-q components of the DG current respectively. Under the balanced network conditions, the above mentioned d-q components are constant quantities.

Fig. 2 presents the block diagram of the DG interface control for constant power operation.The phase-locked loop (PLL), the outer power control loop and the inner current control loop are the three main parts. Based on the input of three single-phase voltages at the PCC, the PLL can offer the voltage phase angle as a benchmark phase to realize synchronous Park transformation and calculate the frequency of the input voltage. In the outer power control loop, PI regulators are introduced to transform the errors between active and reactive power of the DG output and their preset values into the reference values of active and reactive current (i_{dref} and i_{qref}), respectively. In the inner current loop, the errors between the measured and reference d-q values of the DG current are also passed through PI regulators. Meanwhile, the feed-forward compensation from the d-q voltages at the PCC realizes the decoupled control of the d-q components of the DG current as well as the DG active and reactive power output. According to the Park transformation, the output of the inner current control loop (e_d and e_q) is transformed into the voltage reference values of the converter output. Then, the triggering pulses on the inverter switches are gained by sinusoidal pulse-width modulation (SPWM).

When the DG is connected to the utility grid, equations (3) and (4) describe the power flows and the active and reactive power consumed by the RLC load.

$$P_{Load}=P_{DG}+P_{Grid}=3\frac{V_{PCC}^2}{R} \tag{3}$$

$$Q_{Load}=Q_{DG}+Q_{Grid}=3V_{PCC}^2\left(\frac{1}{2\pi fL}-2\pi fC\right) \tag{4}$$

where V_{PCC} and f are the phase voltage at the PCC and its frequency respectively, and RLC represent the load resistance, inductance and capacitance. Thus, equation (4) can also be written in terms of the active power consumption as follows:

$$Q_{Load}=P_{Load}R\left(\frac{1}{2\pi fL}-2\pi fC\right) \tag{5}$$

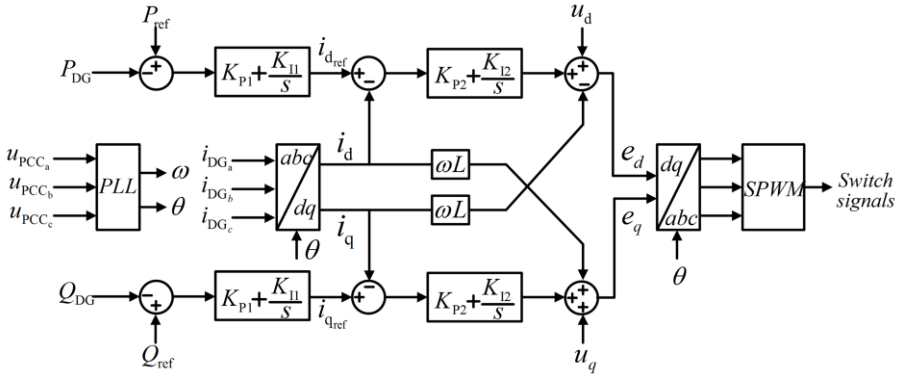

Fig. 2. DG interface control for constant power operation.

It can be inferred from (3) that if P_{Grid} is not zero before the grid disconnection, the PCC voltage will fall or rise during islanding because of the active power mismatch ΔP ($\Delta P = P_{\text{Load}} - P_{\text{DG}}$). Thus, the voltage variation can be utilized to detect the islanding based on the OVP/UVP method and the amount of voltage deviation depends on the value of active power mismatch. If the active power of the DG is set constant, the active power mismatch can be expressed as follows [29]:

$$\Delta P = P_{\text{DG}}\left(\frac{1}{(1+\Delta V)^2} - 1\right) \tag{6}$$

and ΔV can be expressed as:

$$\Delta V = \frac{V_{\text{PCC}}^* - V_{\text{PCC}}}{V_{\text{PCC}}} \tag{7}$$

where V_{PCC} and V_{PCC}^* represent the PCC voltage before and after islanding, respectively.

Similarly, it can be seen from (5) that the amount of deviation in the frequency depends on the values of both active and reactive power mismatches once islanding occurs.The frequency variation also can be used to detect islanding based on the OFP/UFP method. If the DG operates at a unity power factor and there is no active power mismatch during islanding, the reactive power mismatch ΔQ ($\Delta Q = Q_{\text{Load}} - Q_{\text{DG}}$) can be written in terms of the frequency variation as follows [29]:

$$\Delta Q = \frac{3V_{\text{PCC}}^2}{2\pi fL}\left(1 - \frac{f^2}{(f+\Delta f)^2}\right) \tag{8}$$

and Δf can be expressed as:

$$\Delta f = f^* - f \tag{9}$$

where f and f^* represent the PCC voltage frequency before and after islanding, respectively.

However, the relationship between the reactive power mismatch and the frequency variation should be modified when the DG supplies reactive power for the local load. In addition, the impact of the active power mismatch on the frequency deviation should be explored as well for the DG of this kind. Assuming that the DG reactive power output is equal to the load reactive power consumption before islanding, the active power mismatch will change the load reactive power consumption due to the PCC voltage variation during islanding. Thus, it creates the reactive power mismatch between the DG and load to force the PCC voltage frequency to deviate. Since the DG is controlled as a constant power source, the relationship between the active/reactive power mismatch and frequency deviation can be derived as below:

$$\Delta P = -\frac{P_{\text{DG}}(1+4\pi^2 LCf^2)}{f(1-4\pi^2 LCf^2)}\Delta f \tag{10}$$

$$\Delta Q = \frac{Q_{\text{DG}}(1+4\pi^2 LCf^2)}{f(1-4\pi^2 LCf^2)}\Delta f \tag{11}$$

where Δf represents the frequency deviation shown in (9), and f is the PCC frequency before islanding. The detail derivation of the relationship between the active/reactive power mismatch and the frequency deviation can be found in the Appendix. According to (10) and (11), the reactive power mismatch will force the frequency to ascend if ΔQ is above zero during an islanding condition, whereas the frequency will trend to descend with the positive ΔP. The frequency variation caused by the active power mismatch will be offset by that caused by the reactive power in this case. Therefore, whether the frequency eventually rises or drops depends on the amounts of both active and reactive power mismatches. The analysis is the same under the condition that ΔP and ΔQ are both under zero.

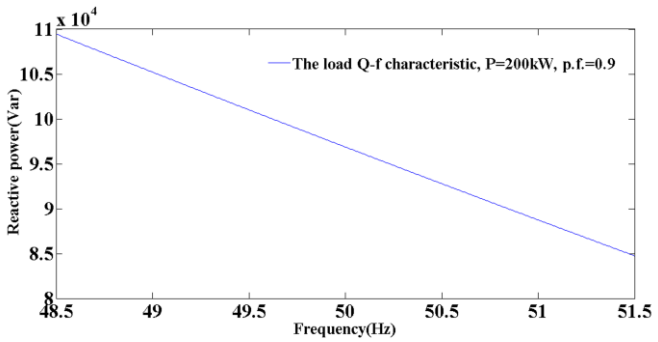

Fig. 3. *Q-f* curve of the load with the power factor equal to 0.9.

For a RLC load whose power factor is 0.9 at 50 Hz with the rated active power 200 kW, Fig. 3 illustrates the load *Q-f* curve whose equation is expressed in (5). It can be seen from Figure.3 that: 1) The load *Q-f* curve shows the approximately linear characteristic for the period between 49.3 Hz and 50.5 Hz; 2) The load *Q-f* curve has a negative slope.The load reactive power consumption is only compensated by the DG after islanding. Thus, the negative slope means that the frequency will be forced to rise if the load reactive power consumption becomes smaller due to the positive ΔQ after islanding, whereas the frequency will drop with the negative ΔQ. Equation (11) gives a detail description of the relationship between the reactive power mismatch and frequency deviation. Reference [20] has also described the load *Q-f* curve equation (5) in terms of the load's resonant frequency (f_0) and quality factor (Q_f) as follows:

$$Q_{\text{load}} = -2P_{\text{load}}\frac{Q_f}{f_0}(f - f_0) \tag{12}$$

and f_0 and Q_f can be expressed as:

$$f_0 = \frac{1}{2\pi\sqrt{LC}} \tag{13}$$

$$Q_f = R\sqrt{\frac{C}{L}} = 2\pi f_0 RC \tag{14}$$

III. Proposed Islanding Detection Algorithm Based on Reactive Power Control

As mentioned in Section II, the active power mismatch will cause voltage deviation once islanding occurs and the OVP/UVP method can be utilized to detect the islanding. Similarly, the frequency deviation depends on the values of both active and reactive power mismatches, and the OFP/UFP method can be used at the same time to detect the islanding effectively. However, if the power mismatches are not large enough, these two passive islanding detection methods will suffer the NDZ due to inadequate changes of the PCC voltage

and its frequency [9], [29]. According to the IEEE Std.929 and IEEE Std.1547, the voltage and frequency thresholds typically range from 0.88 - 1.1 pu and from 49.3 - 50.5 Hz (50 Hz is the rated frequency of the power system), respectively. For a DG rated at 200 kW, the active power mismatch can be created through changing the value of the load resistance. Therefore, if the active power mismatch ranges between -34.7 kW and 58.3 kW according to (6), the islanding will not be detected according to the OVP/UVP method. Similarly, for a RLC load absorbing 200 kW active power and zero reactive power at 50 Hz with quality factor equal to 1 and the DG operating at the unity power factor, the reactive power mismatch can be created through adjusting the value of the load inductance. If there is no active power mismatch during islanding, the OFP/UFP method will fail to detect islanding if the reactive power mismatch ranges between -3.56 kVar and 2.58 kVar from (8) (400 V is the rated line-to-line voltage of the low-voltage power system).

Based on the interface control shown in Fig. 2, the DG can improve the local load power factor and voltage quality by supplying the reactive power. If the DG's reactive power reference value (Q_{ref}) is set equal to the local load's instantaneous reactive power (Q_{load}), the load power factor will be improved to unity. However, the capability of supplying the reactive power for the local load reduces the reactive power mismatch during islanding and the OFP/UFP method will suffer a larger NDZ. The study in [27] has proved that the DG interface control designed for improving the load power factor has no effect on the NDZ active power limits, while the NDZ reactive power limits increase.

There may be both active and reactive power mismatches between the DG and the local load when an islanding condition occurs. According to the study on the relationship between the active/reactive power mismatch and the frequency variation in Section II, the frequency deviations caused by the active and reactive mismatches will be offset by each other when ΔP and ΔQ are either positive or negative simultaneously. Thus, the islanding detection turns to be hard and slow. On the contrary, if ΔP and ΔQ have opposite signs, the frequency will change significantly owing to the same change trends and the islanding can be detected rapidly. In addition, the inverter-based DG is usually configured with the dedicated controller such as the maximum power point tracking controller to dominate the active power output, so that the reactive power control becomes a better choice to realize rapid islanding detection.

Therefore, the proposed reactive power control strategy includes two key points: 1) Creating the reactive power mismatch to eliminate the NDZ and force the frequency to deviate outside the thresholds eventually; 2) Guaranteeing the consistency of the frequency variation trends caused by both active and reactive power mismatches to accelerate the islanding detection speed. To control the DG's reactive power output conveniently, the value of the PCC voltage rather than the active power mismatch can be used as the criterion because the active power mismatch will cause the PCC voltage deviation during islanding.

If the phase voltage at the PCC is greater than or equal to the rated value during islanding, the reactive power reference for the DG can be set as follows:

$$Q_{\text{ref}} = -k_1(f - a) + Q_{\text{load}} \tag{15}$$

where k_1 is a positive value with a being set below the lower frequency threshold 49.3Hz to make Q_{ref} smaller than Q_{load}, and f is the PCC voltage frequency in hertz. For the load shown in Fig. 3, the load Q-f curve and the above DG Q-f curve are simultaneously presented in Fig. 4 with a equal to 49.2. It can be seen from Fig. 4 that wherever the islanding occurs between 49.3 Hz and 50.5 Hz, there will be the reactive power mismatch to force the frequency to increase. With the growing reactive power mismatch, the frequency will eventually deviate outside its upper threshold limit 50.5Hz even if there is no active power mismatch. Therefore, no NDZ will result according to the proposed reactive power control strategy once islanding occurs. In addition, that the PCC voltage rises above the rated value during islanding means the DG offers more active power than the load's active power consumption. Thus, both the active and reactive power mismatches drive the frequency to go up according to (10) and (11), and the islanding can be detected rapidly.

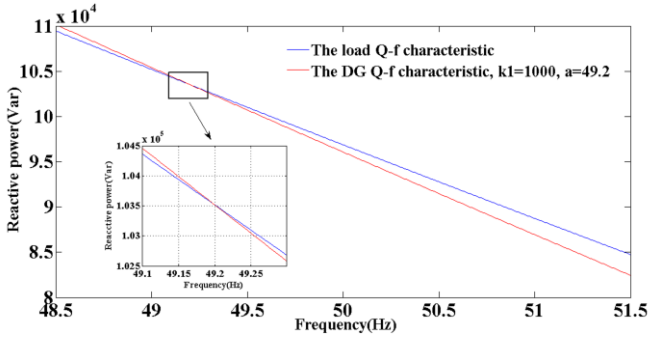

Fig. 4. Q-f curves of the load and the DG when the PCC voltage is greater than or equal to the rated voltage.

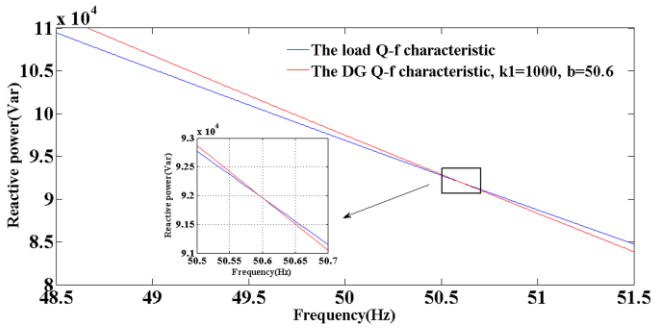

Fig. 5. Q-f curves of the load and the DG when the PCC voltage is lower than the rated voltage.

On the other hand, if the phase voltage at the PCC is smaller than the rated value during islanding, the DG reactive power output will have to supply more reactive power than what the local load needs to strengthen the trend of frequency decrease. The reactive power reference for the DG can be expressed as follows:

$$Q_{\text{ref}} = -k_1(f - b) + Q_{\text{load}} \tag{16}$$

where b is set above the upper frequency threshold 50.5Hz to make Q_{ref} greater than Q_{load}. For the same load condition shown

in Fig. 3 and Fig. 4, Fig. 5 illustrates the load *Q-f* curve and the proposed DG *Q-f* curve with *b* equal to 50.6. It can be inferred that the reactive power mismatch also always exists during islanding to force the frequency to drop until the frequency crosses the UFP threshold value. Similarly, both ΔP and ΔQ make the frequency decrease to accelerate the islanding detection in this situation.

Moreover, one particularly interesting thing is that the proposed reactive power control strategy can also be used to regulate the PCC voltage by forcing the DG to generate different amounts of reactive power in grid-connected condition. The PCC voltage can be calculated approximately by the following equation [21], [26]:

$$V_{\mathrm{PCC}} = V_{\mathrm{Grid}} - \frac{P_{\mathrm{Grid}} R_{\mathrm{g}}}{V_{\mathrm{PCC}}} - \frac{Q_{\mathrm{Grid}} X_{\mathrm{g}}}{V_{\mathrm{PCC}}} \tag{17}$$

where V_{Grid} and $R_{\mathrm{g}} + jX_{\mathrm{g}}$ are the voltage of the grid and the equivalent line impedance at the grid side, respectively. According to the proposed reactive power control strategy, the grid has to supply reactive power for the load ($Q_{\mathrm{Grid}} > 0$) when the voltage is monitored above the rated value. On the other hand, the DG will inject reactive power into the grid except for meeting the load's need ($Q_{\mathrm{Grid}} < 0$) if the voltage drops under the rated value. Thus, the PCC voltage can be regulated based on (17). However, the value of Q_{ref} mainly depends on the preset parameters *k*1, *a*, and *b* in grid-connection condition, so that Q_{Grid} is fixed and generally limited for voltage regulation. To regulate voltage effectively and dynamically, the voltage deviation at the PCC is introduced into the proposed strategy. The improved reactive power control strategy can be obtained as follows:

$$Q_{\mathrm{ref}} = \begin{cases} -(k_1 + \dfrac{V_{\mathrm{PCC}} - V_{\mathrm{N}}}{V_{\mathrm{N}}} \times k_2)(f - a) + Q_{\mathrm{Load}}, V_{\mathrm{PCC}} \geq V_{\mathrm{N}} \\ -(k_1 + \dfrac{V_{\mathrm{N}} - V_{\mathrm{PCC}}}{V_{\mathrm{N}}} \times k_2)(f - b) + Q_{\mathrm{Load}}, V_{\mathrm{PCC}} < V_{\mathrm{N}} \end{cases} \tag{18}$$

where k_2 is also a positive value.

Therefore, the reactive power reference provided by the strategy is a function of the instantaneous reactive power of the load, the PCC voltage and its frequency. All these parameters can be easily obtained and the proposed strategy can take full advantage of the DG by integrating fast islanding detection, load power factor improvement and voltage regulation. It can be inferred from (18) that if the voltage deviation is not large in grid-connected condition, $|Q_{\mathrm{Grid}}|$ will also be small for voltage regulation. Otherwise, the DG will generate much more or much less reactive power for the voltage improvement. What's more, the strategy can guarantee the consistency of the frequency variation trends caused by both active and reactive power mismatches to accelerate the detection, and voltage deviation can further enlarge the reactive power mismatch to realize the islanding detection in less time.

The flowchart of the proposed islanding detection algorithm is presented in Fig. 6. It starts by monitoring the phase voltage at the PCC and measuring the instantaneous Q_{load}. The reactive power control strategy for the DG plays a pivotal role in the algorithm. The value of the reactive power reference for the DG

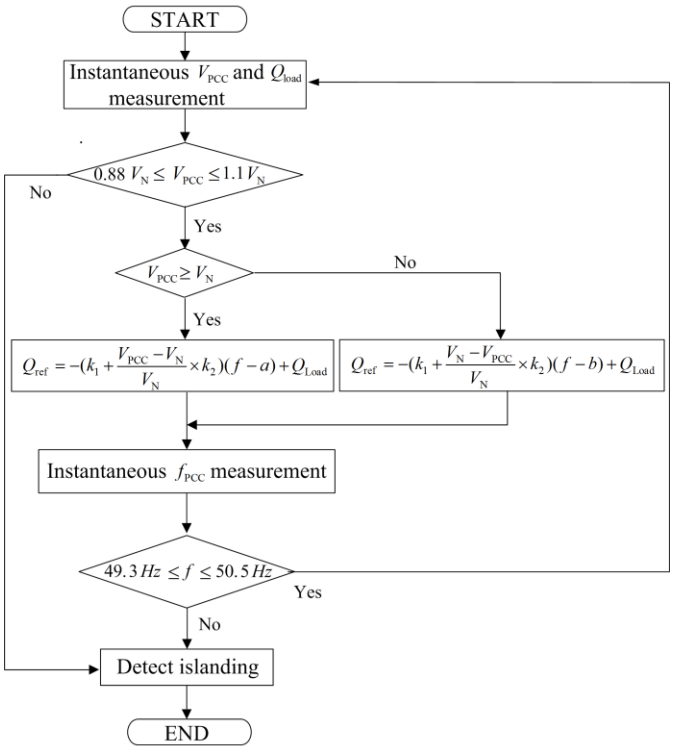

Fig. 6. Flowchart of the proposed algorithm.

depends on the PCC voltage to force the frequency to deviate during islanding or to regulate the PCC voltage in grid-connected mode. If either the frequency exceeds the OFP/UFP threshold limits or the PCC voltage goes across the OVP/UVP threshold values, the islanding will be detected. Moreover, in order to ride through the grid disturbances, loose anti-islanding voltage/frequency trip settings are recommended [21]. Accordingly, the OVP/UVP and OFP/UFP methods will suffer much larger NDZs. However, the proposed strategy can realize the islanding detection effectively and rapidly with the zero NDZ property.

IV. Simulation Results

In this section, several cases are simulated on the power systems computer-aided design (PSCAD) /EMTDC based on the system in Fig. 1. The main system parameters are given in Table I. Adopting the interface control presented in Fig. 2, the DG performs as a constant power source. The DG's active power reference P_{ref} is set to 200 kW and a wide variety of active power mismatch conditions can be created by changing the value of the load resistance. On the other hand, the DG uses the expression (18) as the reactive power reference to generate different amounts of reactive power depending on the measured PCC voltage value. The performance of the proposed islanding detection algorithm is tested under a wide variety of conditions.

A. Comparison of the Performance of the Proposed Reactive Power Control Strategy with Different Values of k_1, k_2, a and b

To check the impact of parameter setting on the strategy performance, five sets of values of parameters k_1, k_2, *a* and *b* shown in Table II are used in (18) when islanding occurs. In

TABLE I
PARAMETERS OF THE STUDY SYSTEM

	parameter	value
Grid	Voltage	400 V
	Frequency	50Hz
	Grid Resistance	0.1 Ω
	Grid Inductance	1.5915mH
DG Inverter Controller	K_{p1}/K_{i1}	0.025/2
	K_{p2}/K_{i2}	1.5/0.01
	P_{ref}	200kW
Load	R	0.8Ω
	L	2.0034mH
	C	3130.4μF
	Q_f	1

TABLE II
PARAMETER SETTING FOR DIFFERENT TEST CASES IN PART *A*

Case	k_1	k_2	a	b	$\|\Delta P\|$ (kW)
1	1000	0	49.2	50.6	0.1
2	1000	0	49	50.8	0.1
3	800	0	49.2	50.6	0.1
4	1000	0	49.2	50.6	5
5	1000	10000	49.2	50.6	5

these five test cases, the values of the load resistance are adjusted to almost absorb the DG's rated output with negligible 0.1 kW mismatch in cases 1, 2, and 3, and to create 5 kW mismatch in cases 4 and 5. Therefore, the frequency deviation is only caused by the reactive power mismatch in the first three cases while the active power mismatch also contributes to the frequency deviation in the following two. The islanding is initiated at t = 0.3 s and the frequency is 50 Hz before islanding.

Fig. 7 illustrates the increasing PCC frequencies due to the negative ΔP during islanding, and Fig. 8 illustrates the dropping PCC frequencies because of the positive ΔP during islanding. It can be noted from Fig. 7 that the islanding can be detected within 66.2 ms in case 1. Compared with case 1, the larger reactive power mismatch due to the smaller a in case 2 forces the frequency to deviate the upper threshold 50.5 Hz in less time, whereas the smaller k_1 in case 3, which means the smaller reactive power mismatch, makes the islanding detection slower. Moreover, the active power mismatch always exists during islanding. With the same k_1, k_2 and a, the islanding detection time in case 4 is 35.4 ms which is shorter than that in case 1. The rapid islanding detection is due to the consistency of frequency variation trends caused by both active and reactive power mismatches. Though k_2 is not set to zero in case 5, the detection time is almost the same as that in case 4. That is because the voltage deviation in both cases, which is caused by the active power mismatch, creates much larger reactive power

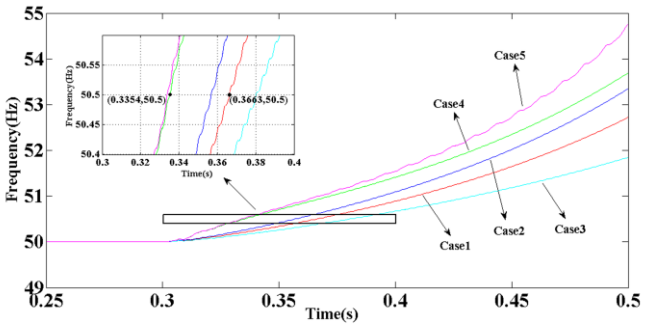

Fig. 7. PCC frequencies with the negative ΔP during islanding.

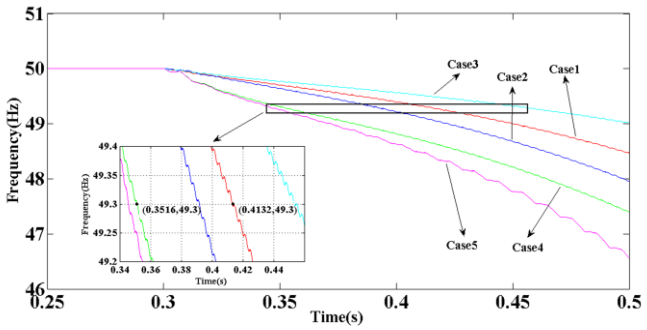

Fig. 8. PCC frequencies with the positive ΔP during islanding.

mismatch and the impact of k_2 on the reactive power mismatch is negligible. However, if the DG size or the active power mismatch is not large, k_2 will accelerate the islanding detection obviously. The analysis of the dropping frequencies shown in Fig. 8 is the same. Therefore, the proposed reactive power control strategy can detect islanding effectively and rapidly. The strategy with larger k_1, k_2, b and smaller a can realize islanding detection in less time.

B. Comparison of the Performance of the Proposed Method with That of the Method in Reference [27]

The islanding detection method in [27] was also designed for the DG generating active and reactive power simultaneously. According to the method, the load reactive power consumption was partly compensated by the DG. The reactive power reference for the DG could be expressed as follows:

$$Q_{ref} = Q_{load} - (Q_{load} + k_3)k_4 \quad (19)$$

where k_3 is in Mvar and k_4 is per unit. Thus, the reactive power mismatch would force the frequency to rise for the inductive load and drop for the capacitive load until the frequency deviated outside the OFP/UFP limits. This part aims to compare the performance of the proposed method in this paper with that of the method mentioned above.

The load reactive power consumption is 96.86 kVar during normal operation in Part *A* (The load's power factor is equal to 0.9 at 50 Hz with the rated active power 200 kW). It can also be 65.74 kVar (p.f. = 0.95) and 20 kVar (p.f. = 0.995) by adjusting the load inductance. All these three kinds of load conditions are analyzed to check the impact of the load reactive power consumption on the performance of the proposed method in this paper and the method in [27]. For each load condition, four

TABLE III
PARAMETER SETTING FOR DIFFERENT TEST CASES IN PART *B*

Case	k_1	k_2	a	b	k_3 (Mvar)	k_4	ΔP (kW)
I	1000	0	49.2	50.6	--	--	-0.1
II	--	--	--	--	0.005	0.01	-0.1
III	--	--	--	--	0.005	0.01	-5
IV	--	--	--	--	0.005	0.01	5

cases are simulated. The parameters for these test cases are shown in Table III. The impact of both parameter setting and the active power mismatch on the proposed method has been illustrated in Part *A*. Therefore, only case I is utilized to compare the performance of the proposed method with that of the method in [27]. The other three cases are all designed to evaluate the performance of the method in [27] with different active power mismatches. For the load consuming reactive power 96.86 kVar, the value of parameter k_4 is set to 0.01 to guarantee that the grid injects almost the same amounts of reactive power during normal operation for both methods. For the other two load conditions, the value of the parameter k_4 is still 0.01 to analyze the performance of the method in [27] under different load conditions.

Fig. 9, Fig. 10, and Fig. 11 illustrate the PCC frequencies for the four test cases under three different load conditions, respectively. As analyzed before, the frequency variation trends caused by active and reactive power mismatches are opposite in some cases. It can be seen from the three figures that the negative ΔP can accelerate the detection and the positive ΔP makes the detection slow according to the method in [27]. However, the proposed method in this paper can make sure that the frequency variation trends caused by active and reactive power mismatches are same during islanding, thus detecting islanding rapidly. The performance is shown in Part *A*. In addition, it can be seen from Fig.9 that islanding can be detected within 82.7 ms according to the method in [27] when the load consumes reactive power 96.86 kVar during normal operation. The islanding detection time is 98.9 ms and 301.3 ms respectively for the other two load conditions. The reactive power mismatch is dependent on the load reactive power consumption. Therefore, the detection becomes slow when the load consumes little reactive power. On the other hand, the reactive power mismatch created by the proposed method in this paper is irrelevant to the load reactive power consumption. It can be seen from the three figures that the islanding can always be detected within a little more than 60 ms. If loose anti-islanding voltage/frequency trip thresholds are set to ride through the grid disturbances, the detection time according to the proposed method in this paper will be much shorter than that based on the method in [27].

C. Extreme Frequency and Load Imbalance conditions

In the extreme circumstances where the frequencies are just the allowable threshold values before islanding, the islanding detection will be slower because of the wider frequency span. Test cases 1 and 4 in Part *A* are utilized to analyze these

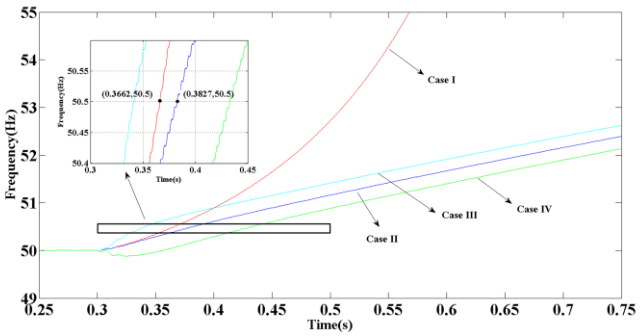

Fig. 9. PCC frequencies for the load normally consuming reactive power 96.86 kVar.

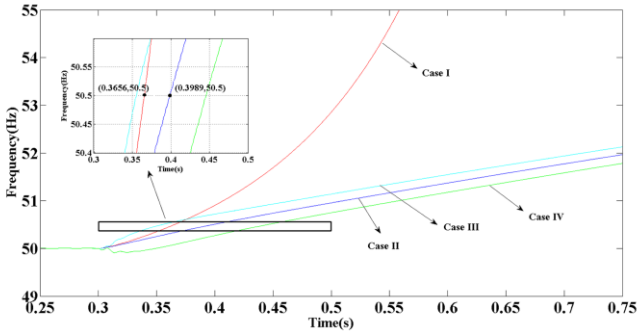

Fig. 10. PCC frequencies for the load normally consuming reactive power 65.74 kVar.

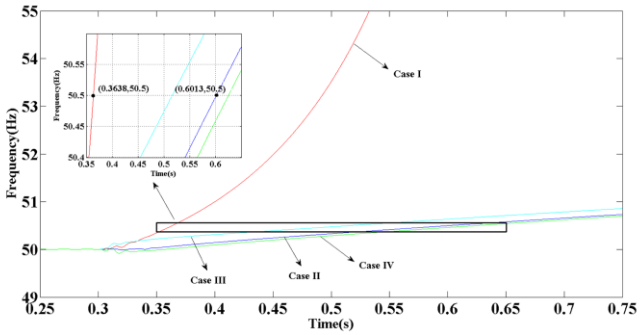

Fig. 11. PCC frequencies for the load normally consuming reactive power 20 kVar.

conditions. It can be seen from Fig. 12 that the islanding can be detected within 278.4 ms when the PCC voltage is above the rated value in case 1. As for case 4, the detection time is 157.8 ms due to the effort of the active power mismatch. Fig. 13 presents the PCC frequencies in both cases when the PCC voltage is below the rated value during islanding. Therefore, even in the extreme circumstances, the detection time is much less than the specified 2 s given in the IEEE Std.1547. As tested in Part *A*, the islanding detection can also be accelerated by adjusting the reactive power control parameters.

As presented in [12], the load imbalance is simulated by varying the load phase resistances. Three cases are considered: 1) In case A, only the resistance of phase a is set to 97% of its rated value; 2) In case B, only the resistance of phase c is set to

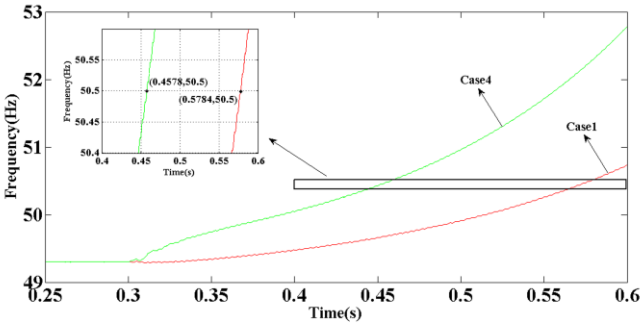

Fig. 12. PCC frequencies for case 1 and case 4 with the system frequency equal to 49.3 Hz before islanding.

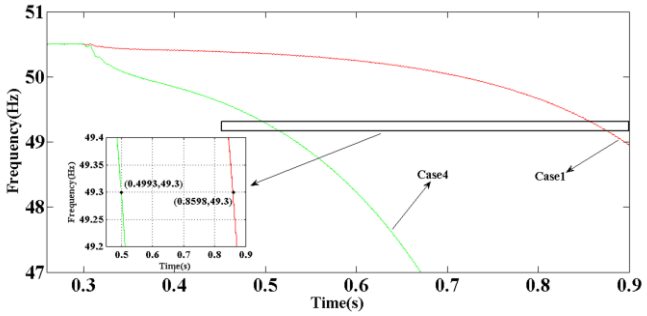

Fig. 13. PCC frequencies for case 1 and case 4 with the system frequency equal to 50.5 Hz before islanding.

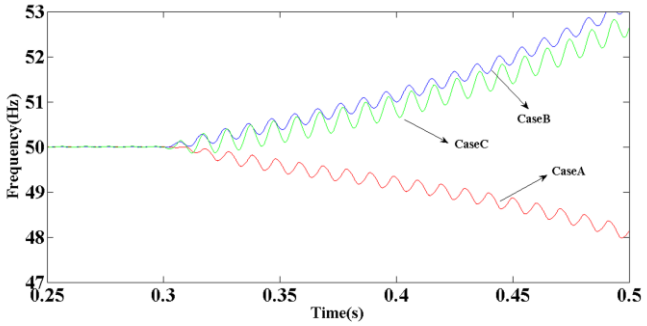

Fig. 14. PCC frequencies for three load imbalance cases.

103% of its rated value; 3) In case C, resistances of phase a and phase c are set at 97% and 103% of the rated value. The values of the reactive power control parameters are the same as those in case 1. Fig. 14 illustrates the PCC frequencies that all deviate outside the thresholds for the three cases. Therefore, the proposed strategy is capable of detecting islanding effectively for load imbalance conditions as well.

D. Performance of the Voltage Regulation in Grid-connected Mode

The performance of the proposed reactive power control strategy to regulate the PCC voltage is tested in this part. To illustrate it clearly, the tests with the DG operating at a unity power factor, fully compensating the load and equipped with the reactive power reference proposed in [27] are conducted as well for comparison. The DG keeps operating in grid-connected mode during the simulation. The undervoltage

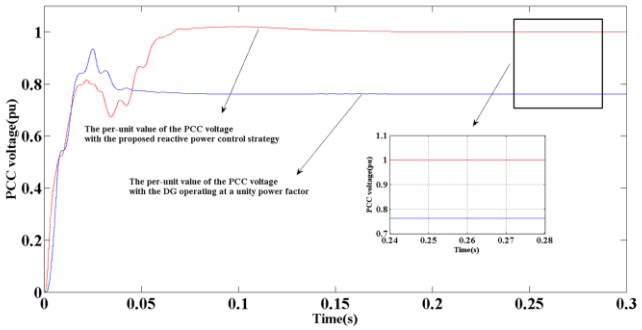

Fig. 15. Per-unit values of the PCC voltage with the proposed reactive power strategy and the DG operating at a unity power factor.

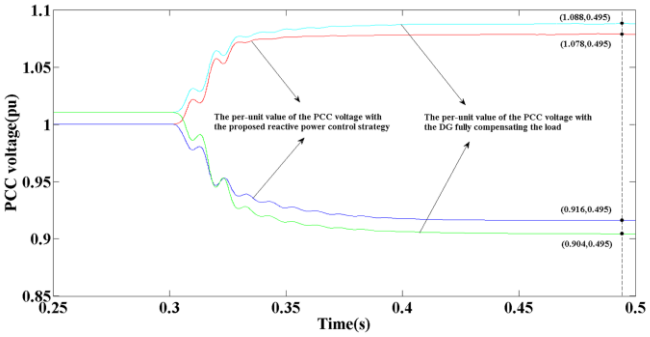

Fig. 16. Per-unit values of the PCC voltage with the proposed reactive power strategy and the DG fully compensating the load.

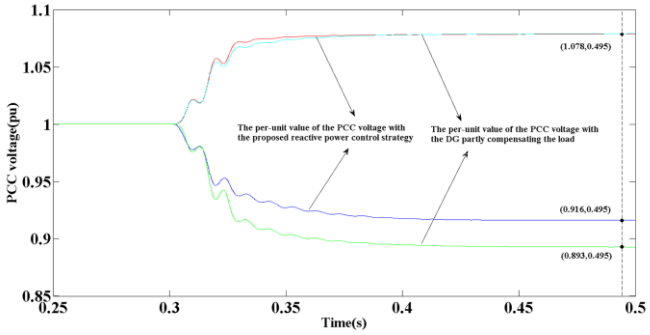

Fig. 17. Per-unit values of the PCC voltage with the proposed reactive power strategy and the method in [27].

or overvoltage at the PCC is simulated by changing the three-phase source voltage (0.88 p.u. and 1.1 p.u. respectively) and is initiated at t = 0.3s. According to the proposed strategy, the rated value of the PCC voltage is a little smaller than 230V (the value of the grid phase voltage) and it is set to 228.3 V. Parameters k_1, k_2 and k_4 are set to 5000, 10000 and 0.04, respectively. According to the proposed strategy and the method in [27], the grid injects almost the same amounts of reactive power before the voltage changes.

When the DG operates at a unity power factor, the grid has to supply reactive power for the load and the PCC voltage drops according to (17). On the other hand, the value of the PCC voltage will keep the same with that of the grid voltage because there is no energy loss on the line impedance, and the load

power factor will be improved to unity if the DG fully compensates the load power. However, the voltage regulation ability only relies on the limited power flow through the line impedance when the grid suffers undervoltage/overvoltage. In addition, the islanding detection suffers a large NDZ with this strategy. As shown in Fig. 15 and Fig. 16, the PCC voltage profile according to the proposed reactive power control strategy is much improved compared with those based on above two strategies. According to the method in [27], the DG compensates part of the load reactive power consumption. Therefore, the PCC voltage profile can be improved when the grid suffers overvoltage. However, the method has a negative effect on the voltage regulation when the grid suffers undervoltage and it may make the PCC voltage even lower according to (17). It can be seen from Fig.17 that: 1) When the grid operates normally or suffers overvoltage, the PCC voltages are almost the same according to the proposed strategy in this paper and that in [27]. It is because almost the same amounts of reactive power are supplied from the DG. 2) When the grid suffers undervoltage, the proposed strategy in this paper performs much better on the voltage regulation than that in [27]. Therefore, the proposed strategy can control the DG to generate different amounts of reactive power to improve the PCC voltage profile dynamically.

E. Multiple-DG Operation

This part presents the performance of the proposed islanding detection algorithm, which is tested on the system with an additional DG. Both DGs are still under constant power control during the detection because whether the islanding occurs or not is unknown. For multiple-DG operation, there are two possible modes of connection between DGs and the local load shown in Fig. 18: 1) Both DGs connect with their own local load respectively and then connect together at the PCC (Mode1); 2) Both DGs connect together with a centralized load at the PCC (Mode2). As for the connection mode 2, when the instantaneous reactive power of the centralized load is acquired as Q_{load}, the proposed reactive power control strategy for each DG should be modified as follows to detect islanding and regulate the voltage:

$$Q_{\text{ref}} = \begin{cases} -(k_1 + \dfrac{V_{\text{PCC}} - V_{\text{N}}}{V_{\text{N}}} \times k_2)(f - a) + \dfrac{Q_{\text{Load}}}{n}, V_{\text{PCC}} \geq V_{\text{N}} \\ -(k_1 + \dfrac{V_{\text{N}} - V_{\text{PCC}}}{V_{\text{N}}} \times k_2)(f - b) + \dfrac{Q_{\text{Load}}}{n}, V_{\text{PCC}} < V_{\text{N}} \end{cases} \quad (20)$$

where n is the number of DGs. The active power mismatch will double during islanding in both connection modes, but the voltage deviation is still the same as that in the single-DG operation condition according to (6). Therefore, the NDZ of the OVP/UVP detection method is unchanged with a large number of DGs, and the key concern is to check whether the frequency will deviate outside the OFP/UFP limits as well with the proposed reactive power control strategy.

Load resistance has to be adjusted to eliminate the impact of the active power mismatch: 1) In connection mode 1, each local load resistance is adjusted to almost consume the DG's rated active power 200 kW with negligible 0.1 kW mismatch; 2) In connection mode 2, the concentrated load resistance is regulated to approximately absorb 400 kW with negligible 0.2 kW mismatch. With the proposed algorithm, Fig. 19 presents the PCC frequencies in the both connection modes. It can be seen that both DGs lose stability. In addition, the islanding can be detected within the same detection time 66.4ms and 115.8ms respectively based on the PCC voltage. That is because the reactive power mismatches in both modes are same during islanding owing to the same reactive power control parameters.

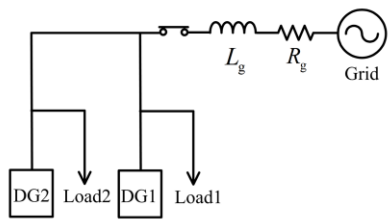

(a)

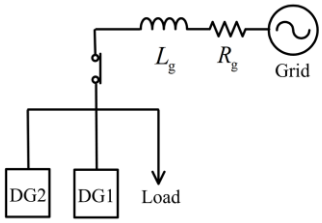

(b)

Fig. 18. Two possible connection modes between DGs and the local load. (a) Connection mode 1. (b) Connection mode 2.

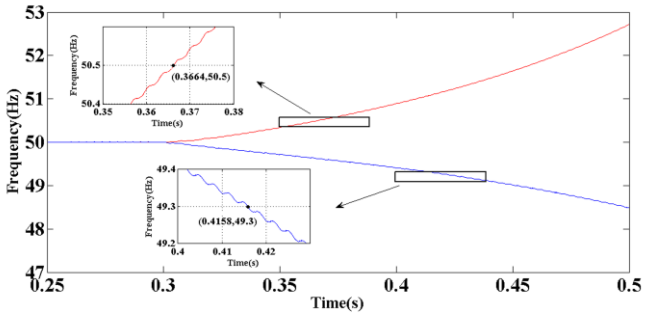

Fig. 19. PCC frequencies with the proposed reactive power control strategy in both connection modes.

In conclusion, the proposed islanding algorithm can also detect islanding rapidly when applied to multiple-DG operation in different connection modes. Moreover, the detection time will be further shortened when the PCC voltage varies due to the active power mismatch. The connection mode 2 also supplies a method to provide sufficient reactive power by offering the needed reactive power from several DGs. Thus, the DGs in this connection mode will perform much better in islanding detection and voltage regulation with more sufficient reactive power generation.

V. Conclusion

The inverter-based DG can generate both active and reactive

power simultaneously under constant power control. For the DG of this kind, this paper analyzes the relationship between the active/reactive power mismatch and frequency deviation respectively during islanding. This paper also presents an innovative islanding detection algorithm for the DG based on reactive power control. In this algorithm, the large voltage deviation due to the sufficient active power mismatch is utilized to detect islanding rapidly according to the OVP/UVP method. To eliminate the NDZ caused by the active power mismatch and detect islanding rapidly, a reactive power control strategy for the DG is proposed to force the frequency to deviate outside the OFP/UFP limits during islanding. Wherever an islanding condition occurs between 49.3 Hz and 50.5 Hz, there will be the reactive power mismatch according to the strategy. With the frequency changing, the mismatch becomes sufficient to drive the frequency to deviate outside the thresholds eventually. Therefore, the OFP/UFP method has the zero NDZ property for the DG equipped with the proposed strategy. Moreover, the reactive power reference for the DG depends on the PCC voltage value that is determined by the active power mismatch during islanding. The consistency of the frequency variation trends caused by both active and reactive power mismatches is guaranteed to accelerate the islanding detection speed. Simulation results verify that the proposed algorithm can detect islanding rapidly.

By introducing the voltage deviation into the strategy, the DG can also dynamically improve the PCC voltage profile especially for the grid with high X_g/R_g lines during normal operation. The islanding detection time is further shortened as well because of the larger reactive power mismatch. Furthermore, the proposed islanding detection algorithm also performs effectively for load imbalance conditions as well as for the system with multiple DGs.

APPENDIX

A. Derivation of the Relationship between ΔP and Δf

Since the DG is controlled as a constant power source, ΔP can be created during islanding by adjusting the value of the load resistance. As mentioned in Section I, when the DG is connected to the utility grid, equation (3) describes the active power consumed by the RLC load. Once islanding occurs, the grid no longer supplies power for the load and the PCC voltage changes due to the active power ΔP. The load active power consumption after islanding can be expressed as follows:

$$P_{\text{Load}} = P_{\text{DG}} = 3\frac{\left[V_{\text{PCC}}(1+\Delta V)\right]^2}{R} \tag{21}$$

The value of ΔP is equal to that of P_{Grid} according to the definition before. Therefore, the following equation can be obtained according to (3) and (21):

$$\frac{P_{\text{DG}}+\Delta P}{V_{\text{PCC}}^2} = \frac{P_{\text{DG}}}{\left[V_{\text{PCC}}(1+\Delta V)\right]^2} \tag{22}$$

This part attempts to analyze the relationship between ΔP and Δf during islanding. Therefore, Q_{Load} is assumed to be equal to Q_{DG} before islanding and the value of Q_{DG} can be expressed as follows:

$$Q_{\text{DG}} = 3V_{\text{PCC}}^2\left(\frac{1}{2\pi fL} - 2\pi fC\right) \tag{23}$$

Since the DG is controlled as a constant power source, Q_{DG} will be the same value after islanding. However, when islanding occurs, the PCC voltage deviation, which is caused by ΔP, makes Q_{Load} change. Thus, the reactive power mismatch exists because of the active power mismatch and the frequency is forced to deviate to make Q_{Load} equal to Q_{DG}. The value of Q_{Load} after islanding can be expressed as follows:

$$Q_{\text{Load}} = 3\left[V_{\text{PCC}}(1+\Delta V)\right]^2\left(\frac{1}{2\pi(f+\Delta f)L} - 2\pi(f+\Delta f)C\right) \tag{24}$$

Then, the following equation can be obtained from (22), (23), and (24):

$$\begin{aligned}(P_{\text{DG}}+\Delta P)\left(\frac{1}{2\pi fL} - 2\pi fC\right) = \\ P_{\text{DG}}\left(\frac{1}{2\pi(f+\Delta f)L} - 2\pi(f+\Delta f)C\right)\end{aligned} \tag{25}$$

Therefore, ΔP can be expressed approximately as (10) in terms of Δf.

B. Derivation of the Relationship between ΔQ and Δf

This part attempts to analyze the relationship between ΔQ and Δf during islanding. Thus, P_{Load} is set to be equal to P_{DG} before islanding. Since the DG is controlled as a constant power source, ΔQ can be created by adjusting the value of the load inductance or/and capacitance. As mentioned in Section II, when the DG is connected to the utility grid, equation (4) describes the reactive power consumed by the RLC load. The value of ΔQ is equal to that of Q_{Grid} according to the definition before. Therefore, the load reactive power consumption before islanding can be expressed in terms of ΔQ as follows:

$$Q_{\text{Load}} = Q_{\text{DG}} + \Delta Q = 3V_{\text{PCC}}^2\left(\frac{1}{2\pi fL} - 2\pi fC\right) \tag{26}$$

Once islanding occurs, the PCC voltage remains the rated value because there is no active power mismatch. On the other hand, the load reactive power consumption is only compensated by the Q_{DG}. Therefore, the reactive power mismatch forces the frequency to deviate until Q_{Load} is equal to Q_{DG}. The load reactive power consumption after islanding can be expressed as follows:

$$Q_{\text{Load}} = Q_{\text{DG}} = 3V_{\text{PCC}}^2\left(\frac{1}{2\pi(f+\Delta f)L} - 2\pi(f+\Delta f)C\right) \tag{27}$$

Then, the following equation can be obtained from (26) and (27):

$$\begin{aligned}Q_{\text{DG}}\left(\frac{1}{2\pi fL} - 2\pi fC\right) = (Q_{\text{DG}}+\Delta Q) \\ .\left(\frac{1}{2\pi(f+\Delta f)L} - 2\pi(f+\Delta f)C\right)\end{aligned} \tag{28}$$

Therefore, ΔQ can be expressed approximately as (11) in terms of Δf.

REFERENCES

[1] H. B. Puttgen, P. R. MacGregor, and F. C. Lambert, "Distributed generation: Semantic hype or the dawn of a new era?" *IEEE Power and Energy Magazine*, vol. 1, no.1 pp. 22–29, Jan-Feb. 2003.

[2] P. P. Barker and R. W. de Mello, "Determining the impact of distributed generation on power systems: Part 1 - Radial distribution systems," in *Proc. IEEE Power Engineering Society Summer Meeting*, Jul. 2000, pp. 1645–1656.

[3] *IEEE Recommended Practice for Utility Interface of Photovoltaic (PV) Systems*, IEEE Standard 929-2000, Apr. 2000.

[4] *IEEE Standard for Interconnecting Distributed Resources with Electric Power Systems*, IEEE Standard 1547-2003, Jul. 2003.

[5] I. J. Balaguer, Q. Lei, S. T. Yang, U. Supatti, and F. Z. Peng, "Control for grid-connected and intentional islanding operations of distributed power generation," *IEEE Trans. Ind. Electron.*, vol. 58, no. 1, pp. 147–157, Jan. 2011.

[6] R. A. Walling, and N. W. Miller, "Distributed generation islanding - implications on power system dynamic performance," in *Proc. IEEE Power Engineering Society Summer Meeting*, Jul. 2002, pp. 92–96.

[7] A. Timbus, A. Oudalov, and N. M. Ho Carl, "Islanding detection in smart grids," in *Proc. IEEE Energy Conversion Congress and Exposition (ECCE)*, Sep. 2010, pp. 3631–3637.

[8] F. De Mango, M. Liserre, A. D. Aquila, and A. Pigazo, "Overview of anti-islanding algorithms for PV aystems. Part I: Passive methods," in *Proc. IEEE Power Electron. Motion Control Conf.*, Aug. 2006, pp. 1878-1883.

[9] Z. Ye, A. Kolwalkar, Y. Zhang, P. Du, and R. Walling, "Evaluation of anti-Islanding schemes based on nondetection zone concept," *IEEE Trans. Power Electron.*, vol. 19, no. 5, pp. 1171–1176, Sep. 2004.

[10] F. De Mango, M. Liserre, and A. D. Aquila, "Overview of anti-islanding algorithms for PV systems. Part II: Activemethods," in *Proc. IEEE Power Electron. Motion Control Conf*., Aug. 2006, pp. 1884-1889.

[11] J. H. Kim, J. G. Kim, Y. H. Ji, Y. C. Jung,and C. Y. Won, "An islanding detection method for a grid-connected system based on the goertzel algorithm," *IEEE Trans. Power Electron.*, vol. 26, no. 4, pp. 1049–1055, Apr. 2011.

[12] H. Karimi, A. Yazdani, and R. Iravani, "Negative-sequence current injection for fast islanding detection of a distributed resource unit," *IEEE Trans. Power Electron.*, vol. 23, no. 1, pp. 298–307, Jan. 2008.

[13] A. Yafaoui, B. Wu, and S. Kouro, "Improved active frequency drift anti-islanding detection method for grid connected photovoltaic systems," *IEEE Trans. Power Electron.*, vol. 27, no.5, pp. 2367–2375, May 2012.

[14] L. A. C. Lopes and H. L. Sun, "Performance assessment of active frequency drifting islanding detection methods," *IEEE Trans. Energy Convers.*, vol. 21, no. 1, pp. 171–180, Mar. 2006.

[15] H. Vahedi and M. Karrari, "Adaptive fuzzy sandia frequency-shift method for islanding protection of inverter-based distributed generation," *IEEE Trans. Power Del*., vol. 28, no. 1, pp. 84–92, Jan. 2013.

[16] G. A. Kern, "SunSine300, utility interactive AC module anti-islanding test results," in *Proc. 26th IEEE Power Photovoltaic Specialists Conference*, Sep. 1997, pp. 1265–1268.

[17] E. J. Estebanez, V. M. Moreno, A. Pigazo, M. Liserre, and A. DellAquila, "Performance evaluation of active islanding - detection algorithms in distributed-generation photovoltaic systems: Two inverters case," *IEEE Trans. Ind. Electron.*, vol. 58, no. 4, pp. 1185–1193, Apr. 2011.

[18] L. A. C. Lopes and Y. Z. Zhang, "Islanding detection assessment of multi-inverter systems with active frequency drifting methods," *IEEE Trans. Power Del*., vol. 23, no. 1, pp. 480–486, Jan. 2008.

[19] M. A. Kashem and G. Ledwish, "Distributed generation as voltage support for single wire earth return systems," *IEEE Trans. Power Del*., vol. 19, no. 3, pp. 1002–1011, Jul. 2004.

[20] H. H. Zeineldin, "A *Q–f* droop curve for facilitating islanding detection of inverter-based distributed generation," *IEEE Trans. Power Electron.*, vol. 24, no. 3, pp. 665–673, Mar. 2009.

[21] Y. Zhou, H. Li, and L. Liu, "Integrated Autonomous voltage regulation and islanding detection for high penetration PV applications," *IEEE Trans. Power Electron.*, vol. 28, no. 6, pp. 2826–2841, Jun. 2013.

[22] J. Zhang, D. H. Xu, G. Q. Shen, Y. Zhu, N. He and J. Ma, "An improved islanding detection method for a grid-connected inverter with intermittent bilateral reactive power variation," *IEEE Trans. Power Electron*., vol. 28, no. 1, pp. 268–278, Jan. 2013.

[23] Y. Zhu, D. H. Xu, N. He, J. Ma, J. Zhang, Y. F. Zhang, G. Q. Shen and C. S. Hu, "A novel RPV (reactive-power-variation) antiislanding method based on adaptive reactive power perturbation," *IEEE Trans. Power Electron.*, vol. 28, no. 11, pp. 4998–5012, Nov. 2013.

[24] P. G. Barbosa, L. G. B. Rolim, E. H. Watanabe, and R. Hanitsch, "Control strategy for grid-connected DC-AC converters with load power factor correction," *IEE Proc.–Generation, Transmission and Distribution*, vol. 145, no. 5, pp. 487–491, Sep. 1998.

[25] S. Huang and F. Pai, "Design and operation of grid-connected photovoltaic system with power-factor control and active islanding detection," *IEE Proc.–Generation, Transmission and Distribution*, vol. 148, no. 3, pp. 243–250, May 2001.

[26] E. Demirok, D. Sera, R. Teodorescu, P. Rodriguez, and U. Borup, "Evaluation of the voltage support strategies for the low voltage grid connected PV generators," in *Proc. IEEE Energy Conversion Congress and Exposition (ECCE)*, Sep. 2010, pp. 710-717.

[27] H. H. Zeineldin, E. F. EI-Saandany, and M. M. A. Salama, "Islanding detection of inverter-based distributed generation," *IEE Proc.–Generation, Transmission and Distribution*, vol. 153, no. 6, pp. 644–652, Nov. 2006.

[28] C. Schauder, and H. Mehta, "Vector analysis and control of advanced static VAR compensators," *IEE Proc.–Generation, Transmission and Distribution*, vol. 140, no. 4, pp. 299–306, Jul. 1993.

[29] H. H. Zeineldin, E. F. EI-Saandany, and M. M. A. Salama, "Impact of DG interface control on islanding detection and nondetection zones," *IEEE Trans. Power Del*., vol. 21, no. 3, pp. 1515–1523, Jul. 2006.

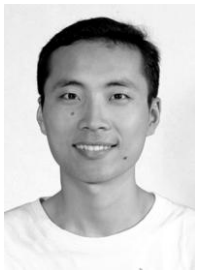

Xiaolong Chen was born in Henan, China, in 1985. He received the B.S. degree and M.S. degree in Electrical Engineering from Tianjin University, China, in 2010 and 2012, respectively.

He is currently working toward the Ph.D. degree in the Department of Electrical Engineering and Automation, Tianjin University, China. His research interests include protection and control of the microgrid and distribution network containing the distributed generation.

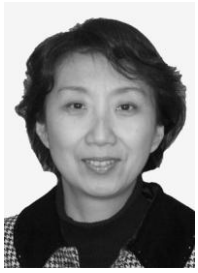

Yongli Li was born in Hebei, China, in 1963. She received the B.S. degree and M.S. degree in Electrical Engineering from Tianjin University, China, in 1984 and 1987, respectively. In1993, she received the Ph.D degree in Electrical Engineering from UniversiteLibre de Bruxelles, Belgium.

She is currently a Professor in the Department of Electrical Engineering and Automation, Tianjin University, and also a member of CIGRE SC-B5. Her research interests include fault analysis of power system and fault diagnosis of electrical equipment, protection and adaptive reclosing of EHV/UHV transmission system, protection and control of the microgrid and distribution network.